J Mater Sci (2009) 44:3387–3392
DOI 10.1007/s10853-009-3448-1

Microwave-assisted metathesis synthesis of Schoenfliesite-type $MSn(OH)_6$ (M = Mg, Ca, Zn, and Sr) materials

Jonathan W. Kramer · Steven A. Isaacs · Venkatesan Manivannan

Received: 14 January 2009 / Accepted: 27 March 2009 / Published online: 9 April 2009

Abstract Technologically important Schoenfliesite type $MSn(OH)_6$ (M = Mg, Ca, Zn, and Sr) materials were synthesized by a simple solid state metathesis (SSM) approach, assisted by microwave energy. The SSM nature of the reaction is strongly suggested by the formation of NaCl byproduct. The synthesized materials are characterized by powder X-ray diffraction (XRD), scanning electron microscopy (SEM), thermo gravimetric analysis (TGA), Fourier transform infrared spectroscopy (FTIR), and diffuse reflectance (DR) in the UV–VIS range, to determine physical properties and establish structure–property relationships for these materials.

Introduction

Compounds with a formula of the form $AB(OH)_6$ are generally known as hydroxide perovskites, and belong to the ReO_3 class of materials having a three-dimensional structural framework that is made up of an array of $B(OH)_6$ octahedra which are corner-shared [1]. A deviation from the ReO_3 structure results in A-site deficient compounds with the stoichiometry $AB(OH)_6$, where, A = Mg, Ca, Sr, or a divalent cation, and B = tetravalent Sn, and accordingly, such compounds are known as Schoenfliesite minerals [2, 3]. The structure was found to have Sn at the 0, 0, 0 positions and Fe at the ½, ½, ½ positions, in space group *Pn3m* with OH groups occupying the $x = 0.056$, $y = 0$, and $z = 0.248$ positions. Because of the similarity in the X-ray diffraction patterns, the compounds belonging to Schoenfliesite minerals were considered to be isostructural.

The unique crystal structures of hydroxide-containing compounds have been explored for several potential applications. It is known that the hydroxyl-bearing perovskite $BaTiO_3$ show good protonic conduction behavior [4]. Jena et al. [5] have shown that the $AB(OH)_6$ compounds that also contain hydroxides have good mobility of protons when the materials are subjected to external thermal energy. Corrosion resistant Mg-based alloys have found application in the automotive and aerospace industries, and accordingly $MgSn(OH)_6$ is used as a protective coating [6]. $CaSn(OH)_6$ is an important intermediate compound during the formation of composite cement [7]. $ZnSn(OH)_6$ has imparted beneficial properties to brominated polyesters in terms of flame retardancy and smoke suppression compared to Sn and Sb-based oxide materials [8]. The anhydrous compounds of these hydroxides also have found several technological usages. Mg-based intermetallics have been studied recently as an alternative to graphite anode material in Li-ion rechargeable batteries [9]. Connor and Irvine [10] synthesized spinel Mg_2SnO_4 as a replacement for possible battery applications. Huang et al. [11] have explored $MgSnO_3$ synthesized by the decomposition of $MgSn(OH)_6$ and found it to have good electrochemical properties. $CaSnO_3$:Sm^{3+} obtained from the corresponding OH compound by high-temperature calcination showed good luminescence properties [12]. Similarly, $ZnSnO_3$ obtained from the parent OH compound showed high sensitivity and selectivity to ethanol as used in the sensor devices [13].

Synthesis procedures

Literature survey indicates $AB(OH)_6$ materials (A = divalent metal and B = tetravalent Sn) have been synthesized by

---

J. W. Kramer · S. A. Isaacs · V. Manivannan (✉)
Department of Mechanical Engineering and Department of Chemistry, Colorado State University, Campus Delivery 1374, Fort Collins, CO 80523, USA
e-mail: mani@engr.colostate.edu

several methods. $MSn(OH)_6$ ($M = Mg$, Mn, Ca, and Fe) were synthesized using a Parr Teflon pressure bomb with reaction time varied between 1 day to several days [2]. Wet sonochemical, co-precipitation, and hydrothermal methods, where proper care needs to be taken to ensure impurities like $Ba(OH)_2$, chloride ions, etc., are avoided, have been reported [14]. A detailed solution-based process involving multiple complex steps to synthesize fine magnesium stannate has been patented [15]. Non-solid state reactions involving precursors where careful control of pH and slow addition of solutions were involved have been reported for $Cd_{1-x}Mg_xSn(OH)_6$, Mg $Sn(OH)_6$, and $MSn(OH)_6$ ($M =$ bivalent metals) [16–19]. $SrSn(OH)_6$ was synthesized by a hydrothermal process where the reaction condition was 180 °C for 16 h [20]. Synthesis of $MSn(OH)_6$ compounds ($M = Ba$ and Sr) using $M(OH)_2$, metal chlorides, and NaOH in a closed batch reactor where a stream of purified and desiccated N_2 was allowed to flow through the system to minimize carbonation with prolonged digestion time was also reported [21]. $ZnSn(OH)_6$ was obtained by a co-precipitation process [22]. A hydrothermal synthesis process was also reported [23, 24]. A surfactant-assisted process where $CaSn(OH)_6$ was obtained, and its calcination lead to $CaSnO_3$ [25]. A solid state reaction where the alkaline–earth oxides were reacted at 1400 °C was also reported [26]. The reported synthesis methods in general involved tedious, time consuming procedures, longer reaction times, proper care to control the reaction condition, etc. A simplified procedure that overcome the disadvantages and further improves the potential usage of the materials is desirable.

Features of metathesis reactions

Self-propagating solid state reactions known as solid state metathesis (SSM) reactions are solvent-less reactions that enable the synthesis of a wide range of technologically important materials in an easy manner. SSM reactions are aided by the formation of NaCl (as a byproduct), which provides the required driving force for the completion of the reaction [27]. SSM reactions can be initiated by using a different source like a heated filament, flames, or by igniting the bulk in a furnace. Several classes of materials, such as metal oxides, carbides, borides, pnictides, and chalcogenides have been synthesized by this approach [27–33].

Using microwave energy to synthesize materials has emerged as a viable alternative for the synthesis of materials, since the application of such a method is faster, more economical, and cleaner [34–38]. We have shown the versatility of this technique by synthesizing several commercially important materials [39]. We have combined the advantages of microwave synthesis of materials with that of the solid state metathesis route to synthesize Schoenfliesite-type $MSn(OH)_6$ metal oxides. The objective of the present work is to synthesize $MSn(OH)_6$ ($M = Mg$, Ca, Sr, and Zn) materials by a metathesis approach assisted by microwave energy, and thus has the advantage of synthesis by a simple procedure. Such a method of synthesis has not been reported previously. The products obtained have controlled morphology, with the desired stoichiometry and a high yield for the reaction. In addition, we have also determined the structural properties of the materials including the optical band gap of the materials.

Experimental

$MgCl_2 \cdot 6H_2O$, $SrCl_2 \cdot 6H_2O$, $CaCl_2 \cdot 6H_2O$, $ZnCl_2 \cdot xH_2O$, and $Na_2SnO_3 \cdot 3H_2O$ obtained from Alfa Aesar, USA, were employed for the preparation of the title compounds. Preparation of $MgSn(OH)_6$ was carried out by reacting $MgCl_2 \cdot 6H_2O$, and $Na_2SnO_3 \cdot 3H_2O$ in a 1:1 molar ratio in a pestle mortar, transferring the resulting mixture to a silica crucible, and subjecting the powders to microwave radiation for 10 min. A domestic microwave operating at 2.45 GHz and 1100 W power was used for the synthesis. No secondary microwave absorbers were used. After the completion of reaction, the powder washed with deionized water and ethanol thoroughly and allowed to dry on a hot plate at 90 °C overnight. XRD of the samples before and after washing were taken. The same procedure was followed for synthesizing other $MSn(OH)_6$ materials ($M = Ca$, Sr, and Zn).

Structural properties of the materials were determined by performing multiple characterizations. X-ray diffraction (XRD) patterns were collected with a Scintag X2 diffractometer using CuK_α radiation. A scan rate of 1°/min with a step size of 0.02° was employed to obtain the XRD spectra. Search match analysis was performed using Bruker EVA software. Fourier Transform infrared spectroscopy (FTIR) measurements in the 400–4000 cm^{-1} range were carried out with a Nicolet Magna FTIR equipped with a deuterated triglycine sulfate detector. Samples for FTIR were made by pressing a mixture of KBr and the powdered sample. A loading of 1–2% was used to obtain FTIR transmission spectra. A total of 512 scans with a resolution of 4 cm^{-1} were used for the specimen and background scans. Thermo gravimetric analysis (TGA) was performed using a weight and temperature-calibrated TA Instruments 2950 instrument under air atmosphere. The sample was heated in a platinum pan with a ramp rate of 10 °C to reach the final temperature. SEM characterization was performed on the JSM-6500F, a field emission system with the in-lens thermal field emission electron gun, and the instrument had Energy Dispersive X-ray Analysis (EDX) capabilities for composition determination. Diffuse reflectance spectra were recorded in the wavelength range 250–2500 nm using a Varian Associates

Cary 500 double beam spectrophotometer equipped with a Praying mantis. Compressed polytetrafluoroethylene was used for standard calibration (100% reflectance). The diffuse reflectance data was used to calculate the absorption coefficient from the Kubelka–Munk (KM) function [40, 41] defined as:

$$F(R_\infty) = \frac{\alpha}{S} = \frac{(1 - R_\infty)^2}{2R} \tag{1}$$

where

$$R_\infty = \frac{R_{\text{sample}}}{R_{\text{PTFE}}} \tag{2}$$

Here α is the absorption coefficient, S the scattering coefficient, and $F(R_\infty)$ is the KM function. The energy dependence of the material in the UV–VIS–NIR was further explored. The energy dependence of semiconductors near the absorption edge is expressed as:

$$\alpha E = K(E - E_g)^\eta \tag{3}$$

Here E is the incident photon energy (hν), E_g is the optical absorption edge energy, "K" is a constant, and the exponent η is dependent on the type of optical transition as a result of photon absorption [42]. The exponent η is assigned a value of 1/2, 3/2, 2, and 3 for direct allowed, direct forbidden, indirect allowed, and indirect forbidden transition, respectively [43]. For the diffused reflectance spectra, the KM function can be used instead of α for estimation of the optical absorption edge energy [42].

Results and discussion

The balanced metathesis reaction between the precursors initiated by microwave radiation is represented as:

$$\begin{aligned} &MgCl_2 \cdot 6H_2O + Na_2SnO_6 \cdot 3H_2O \\ &\quad \rightarrow 2NaCl + MgSn(OH)_6 + 3H_2O \end{aligned} \tag{4}$$

XRD of the as-prepared material was taken, which showed strong intense lines corresponding to a NaCl and $MgSn(OH)_6$ phase. The presence of NaCl strongly indicated that the reaction proceeded in a metathesis way and the formation of such halide salts as by-product is indeed the driving force for the metathesis reaction as demonstrated in the literature [27]. The samples were washed with deionized water many times to remove NaCl and obtain the desired product (Fig. 1). XRD of the washed sample showed the single-phase nature of $MgSn(OH)_6$ by matching with the standard JCPDF 01-074-0366 and accordingly the pattern was indexed. $MgSn(OH)_6$ crystallizes in a *Pmma* space group with cubic lattice parameter $a = 7.77$ Å (Fig. 1b). The XRD of $MgSn(OH)_6$ compound did not have $Mg(OH)_2$ or other impurities like $Mg_4O_3(OH)_2$, $Mg_3O_2(OH)_2$, $Mg_3O(OH)_4$, $Mg_2O(OH)_2$, $Mg_5O_4(OH)_2$, $Mg_5O(OH)_8$, $SrSn(OH)_6$ (Fig. 1a), $ZnSn(OH)_6$ (Fig. 1c), and $CaSn(OH)_6$ (Fig. 1d) compounds were synthesized in the same manner and their single-phase nature was determined in comparison with the standard reference patterns [44]. $ZnSn(OH)_6$ crystallizes in Pn-3(201) space group with cubic lattice parameter of 7.8 Å. However, $SrSn(OH)_6$ crystallizes in hexagonal lattice with $a = 16.35$ Å and $c = 12.34$ Å (JCPDF 00-009-0086) (Pn-3m space group, No 224).

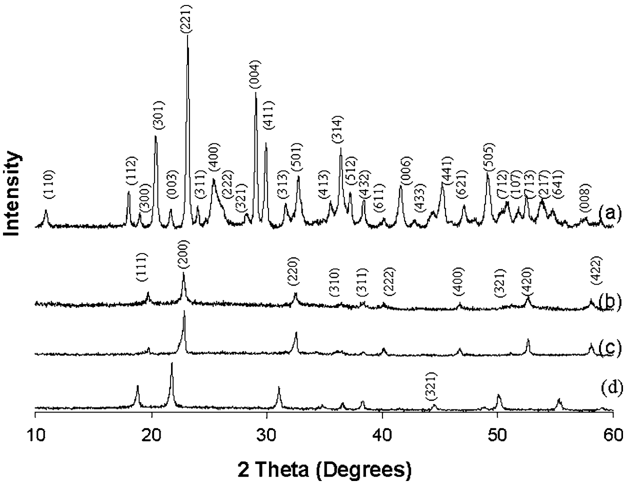

Fig. 1 Powder XRD patterns of $MSn(OH)_6$ materials: M = **a** Sr, **b** Mg, **c** Zn, and **d** Ca

To identify the morphology of the synthesized $(OH)_6$ materials, SEM characterization was performed (Fig. 2). All the hydroxides exhibited well defined morphologies with particle sizes in the sub-micron range as shown for $MgSn(OH)_6$ (Fig. 2a), $CaSn(OH)_6$, (Fig. 2b), $ZnSn(OH)_6$ (Fig. 2c), and $SrSn(OH)_6$ (Fig. 2d). SEM showed controlled morphology (cube, sheet, or rod-like) for $MSn(OH)_6$ particles (M = Mg, Ca, Zn, and Sr). EDX analysis showed the M^{2+}/Sn ratios to be 1.05 (M = Mg), 0.96 (M = Ca), and 1.05 (M = Zn). The corresponding values from AES measurements are 0.98, 1.2, and 0.95, respectively.

Thermal stability of hydroxides

The crystal structure of $MSn(OH)_6$ consists of $Sn(OH)_6$ octahera linked to $Mg(OH)_6$ octahedra with the H atoms disordered over two crystallographic positions within the unit cell. The OH bond in a hydroxyl group is approximately 1 Å in length. The presence of free water in the structure resulted in longer O–H_2 bond distances than were expected [2]. Figure 3 shows the TGA of $MSn(OH)_6$ (M = Mg, Sn, and Ca). The decomposition of these hydroxides is gradual and occurs around 200 °C, resulting in an anhydrous Mg compound (Fig. 2a), according to the reaction:

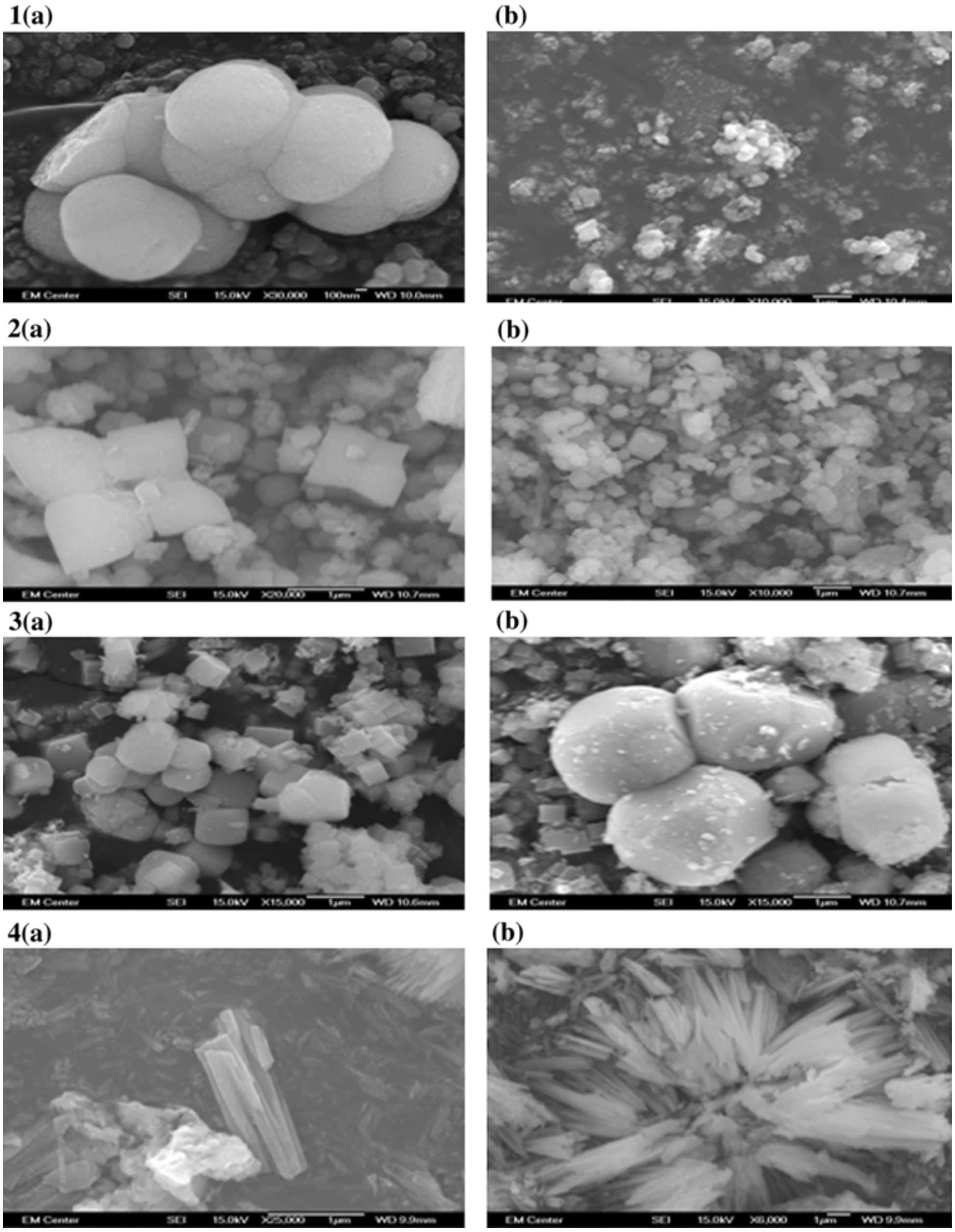

Fig. 2 SEM images of $MSn(OH)_6$ materials: M = (**1**) Mg, (**2**) Ca, (**3**) Zn, and (**4**) Sr (two images for each samples shown)

$$MgSn(OH)_6 \rightarrow MgSnO_3 + 3H_2O \quad (5)$$

$ZnSn(OH)_6$ and $CaSn(OH)_6$ compounds showed a similar behavior with loss of water molecules to produce the corresponding anhydrous compound. The observed weight loss (about 20%) is consistent with the theoretical weight loss (about 22%) [11]. XRD of the heated sample confirmed the anhydrous nature of the compounds.

Figure 4 shows the FTIR of the hydroxides synthesized. FTIR of the samples showed that there is considerable amount of H_2O present in the sample based on the observation of bands at 3200–3300 cm^{-1} [2]. The broadening of peaks is indicative of inclusion of H_2O in the structure and may be ascribed to either O–H bonded to metal ion or O–H in adsorbed H_2O [5]. Peaks around 550 cm^{-1} could arise due to M–O stretching of this type [45].

Lightweight metallic materials are widely used as coatings to impart corrosion protection. The robustness and the integrity of the coatings are determined by corrosion resistant properties. The lifetime of the coatings is correlated to the electronic properties (eg., band-gap) of the material [46]. In order to determine E_g, we have performed the diffuse reflectance spectra of the $(OH)_6$ samples in the UV–VIS–NIR range (Fig. 5). The intercept of the line on abscissa $((F(R_\infty))E = 0)$ gave the value of optical absorption edge energy to be 4.2 ± 0.2 eV for $MgSn(OH)_6$ (Fig. 5, Top). These measurements are consistent with the

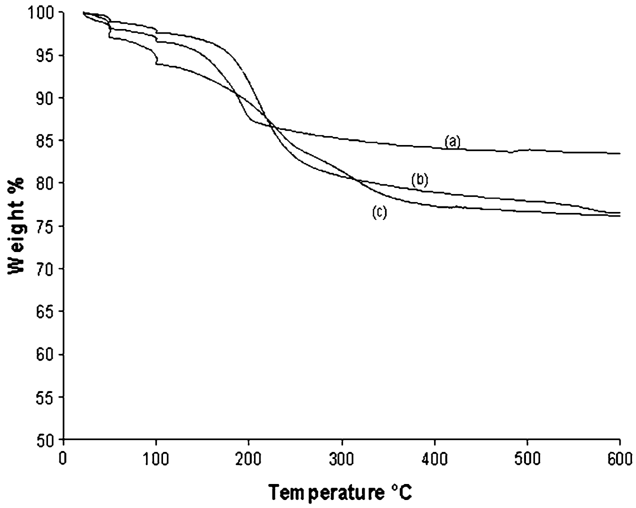

Fig. 3 TGA analysis of $MSn(OH)_6$ materials: M = (a) Ca, (b) Zn, and (c) Mg

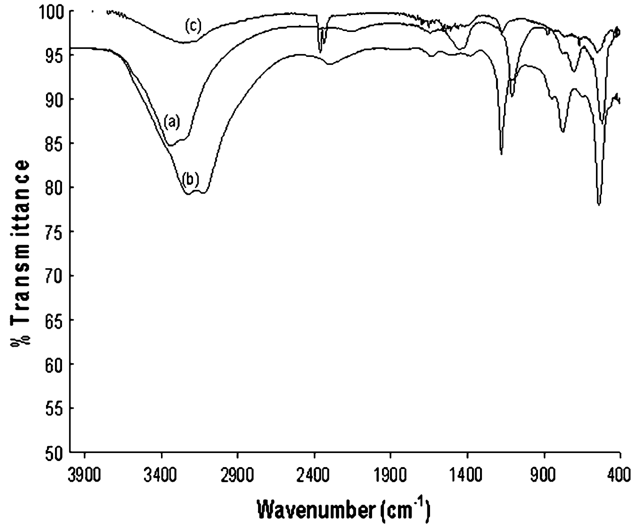

Fig. 4 FTIR of $MSn(OH)_6$ compounds: M = (a) Ca, (b) Zn, and (c) Mg

observation of the photoelectrochemical investigation of conversion coatings on Mg substrates. The insulating nature of these materials could act as passivation layers to protect the coated surfaces predicting an extended life-time [46]. Light absorption edge for $ZnSn(OH)_6$ and $CaSn(OH)_6$ materials were determined in similar way (middle and bottom plots of Fig. 5, respectively).The diffused reflectance spectra for direct band-gap orthorhombic (β) Ta_2O_5 [47] prepared by heating Ta metal in air is also recorded for comparison. The value of optical absorption edge energy for indirect allowed transition for Ta_2O_5 was found to be 4.0 ± 0.2 eV which is consistent with those obtained for β-Ta_2O_5 [48].

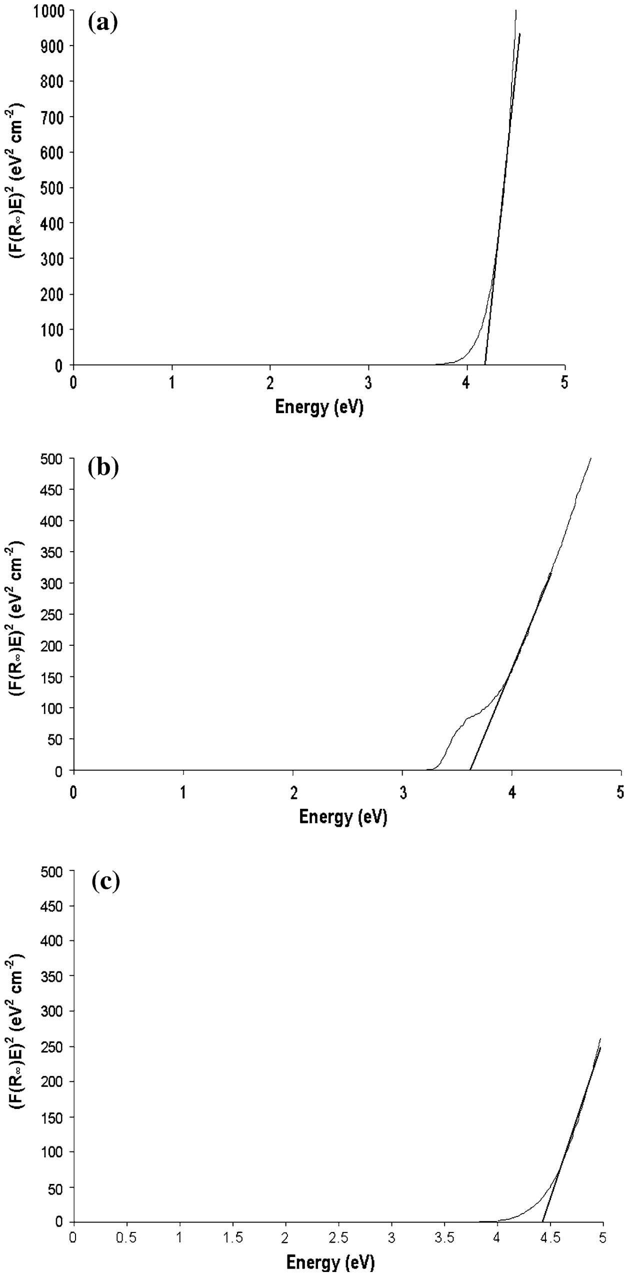

Fig. 5 **a** Plot of $F(R_\infty)$ vs. E (eV) for (**a**) the estimation of the optical absorption edge energy for $MgSn(OH)_6$, **b** Plot of $F(R_\infty)$ vs. E (eV) for the estimation of the optical absorption edge energy for $ZnSn(OH)_6$, and **c** Plot of $F(R_\infty)$ vs. E (eV) for the estimation of the optical absorption edge energy $CaSn(OH)_6$

Conclusions

A simple, convenient method of synthesizing single-phase materials of $MSn(OH)_6$ (M = Mg, Ca, Zn, and Sr) is proposed which has several advantages, such as being less-labor intensive and having a greater potential for easy scale-up, compared with known methods of syntheses. Low-temperature treatment (~300 °C heating) of the materials resulted in the formation of corresponding anhydrous materials. The optical band-gaps of the materials determined are indicative of the insulating nature of the materials and position them as potential protective coatings for metal surfaces.

Acknowledgements The authors would like to acknowledge Prof. Allan Kirkpatrick, Department Head, Mechanical Engineering, Colorado State University, for his continued help, encouragement, and support.

References

1. Bock O, Muller U (2002) Z Anorg Allg Chem 628:987
2. Basciano LC, Peterson RC, Roeder L, Swainson I (1998) Can Mineral 36:1203
3. Trunz HS, Contag B (1960) Acta Crystallogr 12:601
4. Jena H, Kutty KVG, Kutty TRN (2004) Mater Res Bull 39:4
5. Jena H, Kutty KVG, Kutty TRN (2004) Mater Chem Phys 88:167
6. Barchiche C, Rocca EE, Hazan J (2008) Surf Coat Technol 202:4145
7. Hill J, Sharp H (2005) J Am Ceram Soc 88(3):560
8. Kicko-Walczak E (1999) Polym Degrad Stab 64(3):439
9. Moriga T, Watanabe D, Tsuji D, Massaki S, Nakabayashi J (2000) J Solid State Chem 153:386
10. Connor PA, Irvine JTS (2001) J Power Sources 97–98:223
11. Huang F, Yuan Z, Zhan Y, Zhou J (2004) Mater Chem Phys 83:16
12. Bingfu L, Li B, Zhang H, Li W (2007) Opt Mater 29(11):1491
13. Xu J, Yanli L, Xiu X (2002) Guisuanyan Xuebao 30(3):321
14. Inagaki T, Kuroishi T, Yamashita M, Urata M (2004) Z Anorg Allg Chem 527(8):193
15. Sony Corporation (1985) Jpn Kokai Tokkyo Koho, Japanese Patent JP 60071525
16. Levy-Clement C, Morgenstern-Badarau I, Yves M, Michel A (1968) Comptes Rendus des Seances de l'Academie des Sciences, Series C: Sciences Chimiques 266(11):790
17. Levy-Clement C, Morgenstern-Badarau I, Yves M, Michel A (1967) Comptes Rendus des Seances de l'Academie des Sciences Series C: Sciences Chimiques 265(11):585
18. Morgrenstern-Badarau I, Yves M, Poix P, Michel A (1965) Compt Rend 260(13):3668
19. Ramamurthy P, Secco EA (1971) Can J Chem 49:2113
20. Chen Di, Jinhua Ye (2007) Chem Mater 19:4585
21. Leoni M, Viviani M, Nanni P, Buscaglia V (1996) J Mater Sci Lett 15:1302
22. Yuan Z, Huang F, Sun J, Sun Y (2002) Chem Lett 43:408
23. Lu Z, Tang Y (2005) Mater Chem Phys 92:5
24. Zhang Y, Guo M, Zhang M, Yang C, Ma T, Wang X (2007) J Cryst Growth 308:99
25. Lu Z, Wang Y, Li J (2004) J Solid State Chem 177:3075
26. Azad AM, Shyan LLW, Yen PT (1999) J Alloys Compd 282:109
27. Bonneau PR, Jarvis RF, Kaner RB (1991) Nature 349:510 (and references therein)
28. Wiley JB, Gillan EG, Kaner RB (1991) Nature 349:510
29. Gillan EG, Kaner RB (2001) J Mater Chem 11(7):1951 (and references therein)
30. Nartowski AM, Parkin IP, MacKenzie M, Craven AJ, Macleod I (1999) J Mater Chem 9:1275
31. Gopalakrishnan T, Sivakumar K, Ramesha K, Thangadurai V, Subbabba GN (2000) J Am Chem Soc 122(26):6237 (and references therein)
32. Mandal TK, Gopalakrishnan J (2004) J Mater Chem 14(8):1273
33. Parkin IP (1996) Chem Soc Rev 199 (and references therein)
34. Ramesh PD, Rao KJ (1995) Adv Mater 7:177
35. Vaidhyanathan B, Ganguli M, Rao KJ (1995) Mater Res Bull 30:1173
36. Parhi P, Ramanan A, Ray AR (2007) J Am Ceram Soc 90:1237
37. Parhi P, Ramanan A, Ray AR (2004) Mater Lett 58:3610
38. Parhi P, Ramanan A, Ray AR (2006) Mater Lett 60:218
39. Parhi P, Kramer JW, Manivannan V (2008) Mater Sci Eng B 153:53 (and references therein)
40. Kubelka P, Munk F (1931) Z Tech Phys 12:593
41. Kortun G (1969) Reflectance spectroscopy principles method applications. Springer Verlag, New York
42. Barton DG, Shtein M, Wilson RD, Soled SL, Iglesa E (1999) J Phys Chem B 103:630
43. Tauc J, Grigorov R, Vancu A (1966) Phys Status Solidi 15:627
44. JCPDF files $CaSn(OH)_6$: 00-009-0030, and $ZnSn(OH)_6$: 01-073-2384, and $SrSn(OH)_6$: 00-009-0086 ICDD, PCPDFWIN v.2.1, JCPDS—International Centre for Diffraction Data (2000)
45. Nakamoto K (1997) Infrared and raman spectra of inorganic and coordination compounds, vol B. Wiley, New York, p 57
46. Anicai L, Masi R, Santamaria M, Di Quarto F (2005) Corros Sci 47:2883
47. Sahu BR, Kleinman L (2004) Phys Rev B 69:165202
48. Knausengerger WH, Tauber RN (1973) J Electrochem Soc 129:927